ASPECTS OF TANDEM BOGIE AXLES FROM PERSPECTIVE OF STATE-SPACE MODELING

Martin Maloch, Stefan Cornak
University of Defence in Brno, Czech Republic
martin.maloch@unob.cz, stefan.cornak@unob.cz

Abstract. The main differences between tracked and wheeled vehicles are the cross-country capability, dependability, comfort, travel speed for the paved surfaces (roads) and last but not least – the amount of resistance which needs to be overcome in order to move the vehicle or its energy efficiency. In the past decade, these differences are growing thinner in favour of wheeled vehicles, due to clever design and modern technologies that enabled torque vectoring and suspension types that are far beyond the coil springs and ordinary dampers. The developments are so quick that somehow some designs are skipped and replaced by others, even before we reached its maximal potential. One such example are the leaf springs, the very old design which has its powerful benefits for the heavy trucks. Currently the researchers are focused on the enhancements for the material point of view, spring steel is being replaced by various composite materials, so it weighs less, its behaviour is more controllable and the unsprung mass is lower.But the power of the leaf spring lies elsewhere – it is its utilization for the tandem suspensions, often called the tandem bogie, or walking beam – the leaf spring as the beam or equalizing suspension. For the driven axles, this layout greatly enhances the cross-country capability of wheeled vehicle, since it is able to equally distribute the normal forces, therefore the driving forces are higher and the vehicle can better move. This system works really well in real life muddy conditions, however, it is very complex for the simulations and modelling. Firstly, the leaf spring as it is and its dynamic nonlinear hysteretic behaviour is extremely complex, secondly, its implementation to the dynamic simulation is rather challenging. This paper will provide the insight to the differences between the independent suspension and the tandem one, from the perspective of the state-space models with 8 and 9 degrees of freedom.

Keywords: state-space models, tandem layout.

Introduction

There are two options for answer to the question “Why is it important to know how the vehicle behaves in the difficult terrain/conditions?”, firstly, for the purpose of further research and development, secondly, for the real-time simulation – can the vehicle travel from point A to B on first route, second or third? First being the longest on paved surface, second relatively short with medium terrain obstacles and third being the shortest, but with rough conditions. How fast can the vehicle travel, how much fuel will be burnt, can the vehicle finish the journey without being stuck, can the crew take the journey, or will they develop motion sickness? With modern technology on a current level, the 3D map of a specific terrain can be made easier than we might think, with the utilization of drones.So, the second option for the first question is relatively close to be actual.

Of course, there will be constants and coefficients which are gradually changing, therefore only the range of the values will be known. The simulation in only as good as are the inputs for it. Some simulations can be very precise, but they are extremely time consuming in a range of hours. Sometimes, the decision about which route to take must be made in terms of minutes.

This paper is a part of a bigger project, which is the creation of the full vehicle simulation. The first step should be the recognition of the coefficients and constants, which are hard to set, or unknown, or can cause trouble during the simulation. The complexity of the simulation rises with the number of nonlinear coefficients. In terms of vehicles, the first simulation or analysis is the quarter car model with two vertical degrees of freedom (DOF) [1]. The next step is 4 DOF, two vertical motions for unspung masses, one vertical motion for sprung mass and a pitch motion of sprung mass [2]. These basic models are frequently used for quick analysis of the basic behaviour. Lot of modern suspension controllers are created on these two simplest models [3]. The dampers are main focus of many researchers [4], since their controllability has a big potential. They prefer the 2 and 4 DOF models due to their simplicity, easy debugging and relatively good evaluation of the results. Mostly, the aforementioned models utilize the linear spring models, which represent coil springs. For more complexity, the variable stiffness rate can be implemented. The leaf springs, on the other hand, are far more complex, mainly due to their hysteretic and nonlinear behaviour. With the knowledge of the material and the free geometry, the stiffness rate of the coil spring can be easily found by the finite element analysis. However, for the leaf spring there are many factors, which must be taken into

account [5]. The simplest model of the leaf spring is the SAE three link [6], although it is hard to cover the multi-leaf spring with this model. The presented model provides the baseline for the future comparison of the results with the more complex dynamic model, primal results from this simulation can serve as the guideline for the troubleshooting of the multibody dynamic model. The main advantage over the dynamic simulation is the simulation time and shorter preparation time. The main disadvantage is the precision of the results and lack of ability of gaining the other vehicle related results.

8 DOF vehicle model

The aforementioned bigger project is the analysis of the vehicle in Fig. 1, due to its presence in the university grounds, every important part of the 3D model is based on the real part. Some parts, like the engine, have only the illustrative purpose – but it has the weight and dimensions of the real one. The 3D model is important for the knowledge of the position of the centre of gravity (COG) and weights of the sprung/unsprung masses along with their respective moments of inertia.

Fig. 1. **3D Model of the 6x6 vehicle Tatra T810 with the cargo**

The first mathematical model will be the half car version of this particular truck, only with the independent rear suspensions, not the tandem one. Every constant and coefficient is based on the value from the 3D model of the vehicle, or from other simulation. The model will be excited by a simple bump function, presented in Fig. 2. The transition between a straight line and slope is as smooth as possible, to prevent any unwanted steep rises in the state-space system.

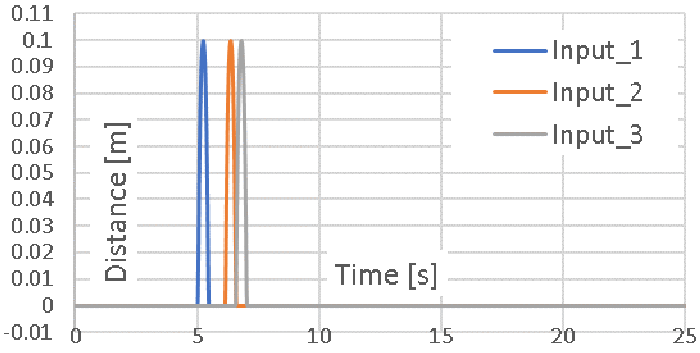

Fig. 2. **Excitation data for the models**

Presented in Fig. 3 is the arrangement of the half-truck suspension system, where the pitch axis moment of inertia of the chassis is I_{ch} and I_c for the cabin (kg·m^2), $k_{S1,2,3}$ is the suspension stiffness for the first, second or third axle, k_S is the driver seat spring stiffness, $k_{t1,2,3}$ is the tire stiffness for the wheels, $k_{C1,2}$ for the cabin suspension stiffness N·m^{-1}, $c_{S1,2,3}$f or the suspension damping coefficient, c_s

for the driver seat damping coefficient, $c_{C1,2}$ for the cabin damping coefficient (N·s·m^{-1}) and COG$_{ch,c}$ stands for the centre of gravity of the chassis, respectively the cabin. The other labels stand for: $x_{w1,2,3}$ vertical displacements of the unsprung masses of the axles, represented as wheels (m), $\dot{x}_{w1,2,3}$ for the velocity of the unpsrung masses (m·s^{-1}) and $\ddot{x}_{w1,2,3}$ fort its acceleration respectively (m·s^{-2}) , x_{ch} for the vertical displacement of the COG of the chassis (m), $\dot{x}_{ch}$ for its velocity (m·s^{-1}) and $\ddot{x}_{ch}$ acceleration (m·s^{-2}), φ is for the pitch angle of the chassis (rad), $\dot{\varphi}_{ch}$ is for its angular velocity (rad s^{-1}), $\ddot{\varphi}_{ch}$ for its angular acceleration (rad s^{-2}), x_C for the vertical displacement of the COG of the cabin (m), $\dot{x}_C$ for its velocity (m·s^{-1}) and $\ddot{x}_C$ acceleration (m·s^{-2}), φ_C is for the pitch angle of the cabin (rad), $\dot{\varphi}_C$ is for its angular velocity (rad·s^{-1}) and $\ddot{\varphi}_C$ for its angular acceleration (rad s^{-2}), $x_{ch1,2,3}$ is for the chassis displacements (m) in the regions where it meets with suspension links, $\dot{x}_{ch1,2,3}$ is for its velocity (m·s^{-1}), $x_{C1,2}$ is for the cabin displacements (m) in the regions where it meets with the chassis, $\dot{x}_{C1,2}$ is for its velocity (m·s^{-1}), $x_{chC1,2}$ is for the chassis displacements (m) in the regions where it meets with the cabin, $\dot{x}_{chC1,2}$ is for its velocity (m·s^{-1}). The rest of the labels are the distances (m) according to Fig. 3.

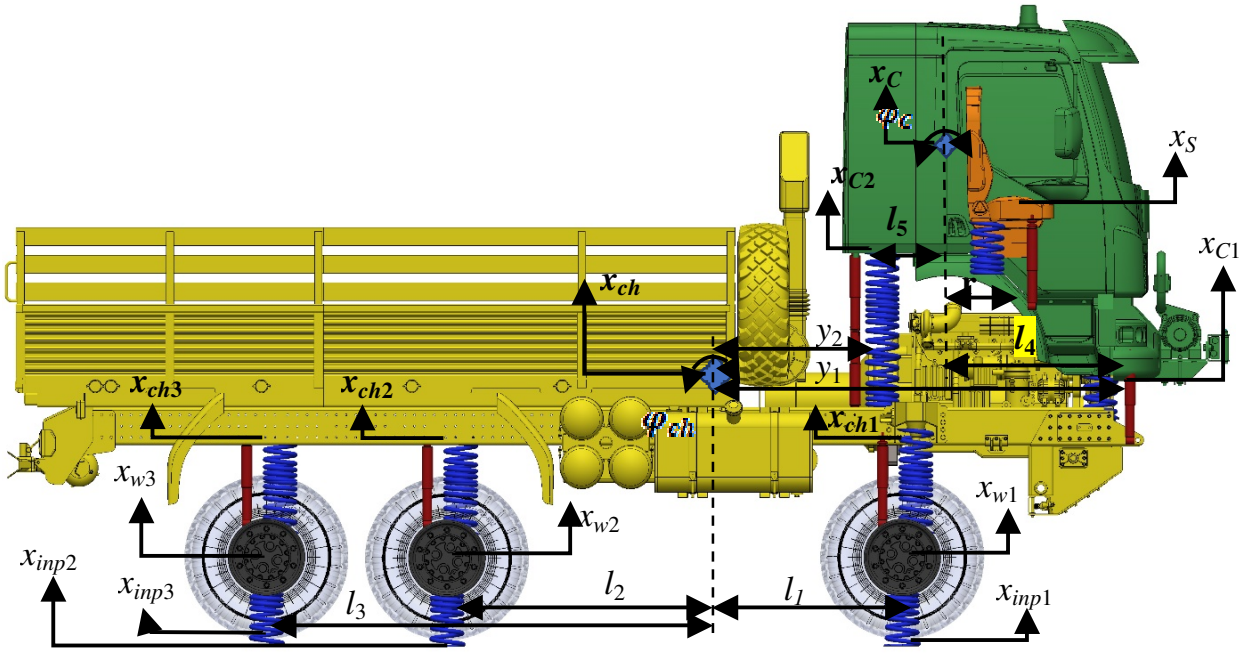

Fig. 3. **Half truck schematic system:** seat mass m_s (orange), cabin mass m_c (green), chassis mass m_{ch}(yellow), unsprung mass (wheels and suspension links) $m_{w1,2,3}$ (black) in kg, spring elements (blue) and damper elements (red), ◆ – COG of the marked part

With utilization of the Newton's second law of the motion on the system in Fig. 3, eight equations of motion were obtained (1- 8):

$$m_{ch}\cdot\ddot{x}_{ch} = k_{S1}\cdot(x_{w1} - x_{ch1}) + c_{S1}\cdot(\dot{x}_{w1} - \dot{x}_{ch1}) + k_{S2}\cdot(x_{w2} - x_{ch2}) +$$
$$+ c_{S2}\cdot(\dot{x}_{w2} - \dot{x}_{ch2}) + k_{S3}\cdot(x_{w3} - x_{ch3}) + c_{S3}\cdot(\dot{x}_{w3} - \dot{x}_{ch3}) - k_{C1}\cdot(x_{chC1} - x_{C1}) -$$
$$- c_{C1}\cdot(\dot{x}_{chC1} - \dot{x}_{C1}) - k_{C1}\cdot(x_{chC2} - x_{C2}) - c_{C2}\cdot(\dot{x}_{chC2} - \dot{x}_{C2}), \quad (1)$$

$$I_{ch}\cdot\ddot{\varphi}_{ch} = l_1\cdot k_{S1}\cdot(x_{w1} - x_{ch1}) + l_1\cdot c_{S1}\cdot(\dot{x}_{w1} - \dot{x}_{ch1}) - l_2\cdot k_{S2}\cdot(x_{w2} - x_{ch2}) -$$
$$- l_2\cdot c_{S2}\cdot(\dot{x}_{w2} - \dot{x}_{ch2}) - l_3\cdot k_{S3}\cdot(x_{w3} - x_{ch3}) - l_3\cdot c_{S3}\cdot(\dot{x}_{w3} - \dot{x}_{ch3}) - l_4\cdot k_{C1}\cdot(x_{chC1} - x_{C1}) -$$
$$- l_4\cdot c_{C1}\cdot(\dot{x}_{chC1} - \dot{x}_{C1}) + l_5\cdot k_{C2}\cdot(x_{chC2} - x_{C2}) + l_5\cdot c_{C2}\cdot(\dot{x}_{chC2} - \dot{x}_{C2}), \quad (2)$$

$$m_c\cdot\ddot{x}_c = k_{C1}\cdot(x_{chC1} - x_{C1}) + c_{C1}\cdot(\dot{x}_{chC1} - \dot{x}_{C1}) + k_{C2}\cdot(x_{chC2} - x_{C2}) +$$
$$+ c_{C2}\cdot(\dot{x}_{chC2} - \dot{x}_{C2}) - k_s\cdot(x_{Cs} - x_S) - c_S\cdot(\dot{x}_{Cs} - \dot{x}_S), \quad (3)$$

$$I_c\cdot\ddot{\varphi}_c = l_4\cdot k_{C1}\cdot(x_{chC1} - x_{C1}) + l_4\cdot c_{C1}\cdot(\dot{x}_{chC1} - \dot{x}_{C1}) - l_5\cdot c_{C2}\cdot(x_{chC2} - x_{C2}) -$$
$$- l_5\cdot c_{C2}\cdot(\dot{x}_{chC2} - \dot{x}_{C2}) - r\cdot k_s\cdot(x_{Cs} - x_S) - r\cdot c_S\cdot(\dot{x}_{Cs} - \dot{x}_S), \quad (4)$$

$$m_s\cdot\ddot{x}_s = k_s\cdot(x_{Cs} - x_S) - c_S\cdot(\dot{x}_{Cs} - \dot{x}_S), \quad (5)$$

$$m_{w1}\cdot\ddot{x}_{w1} = k_{t1}\cdot(x_{inp1} - x_{w1}) - k_{S1}\cdot(x_{w1} - x_{ch1}) - c_{S1}\cdot(\dot{x}_{w1} - \dot{x}_{ch1}), \quad (6)$$

$$m_{w2}\cdot\ddot{x}_{w2} = k_{t2}\cdot(x_{inp2} - x_{w2}) - k_{S2}\cdot(x_{w2} - x_{ch2}) - c_{S2}\cdot(\dot{x}_{w2} - \dot{x}_{ch2}), \quad (7)$$

$$m_{w3}\cdot\ddot{x}_{w3} = k_{t3}\cdot(x_{inp3} - x_{w3}) - k_{S3}\cdot(x_{w3} - x_{ch3}) - c_{S3}\cdot(\dot{x}_{w3} - \dot{x}_{ch3}), \quad (8)$$

where $x_{ch1} = x_{ch} + l_1\cdot\varphi_{ch}$, $x_{ch2} = x_{ch} + l_2\cdot\varphi_{ch}$, $x_{ch3} = x_{ch} + l_3\cdot\varphi_{ch}$,
$x_{C1} = x_C + l_4\cdot\varphi_C$, $x_{C2} = x_C + l_5\cdot\varphi_C$,
$x_{chC1} = x_{ch} + y_1\cdot\varphi_C$, $x_{chC2} = x_{ch} - y_2\cdot\varphi_C$, $x_{Cs} = x_C + r\cdot\varphi_C$.

These equations were solved with utilization of Matlab/Simulink, according to the guidelines for the state-space models at [7]. The Simulink diagram is presented in Fig.4. The input for the analysis was the spreadsheet with time and data points for all of the three inputs according to Fig. 2. The output data were saved and then through the script exported to spreadsheet, were further analytical and graphic work was conducted.

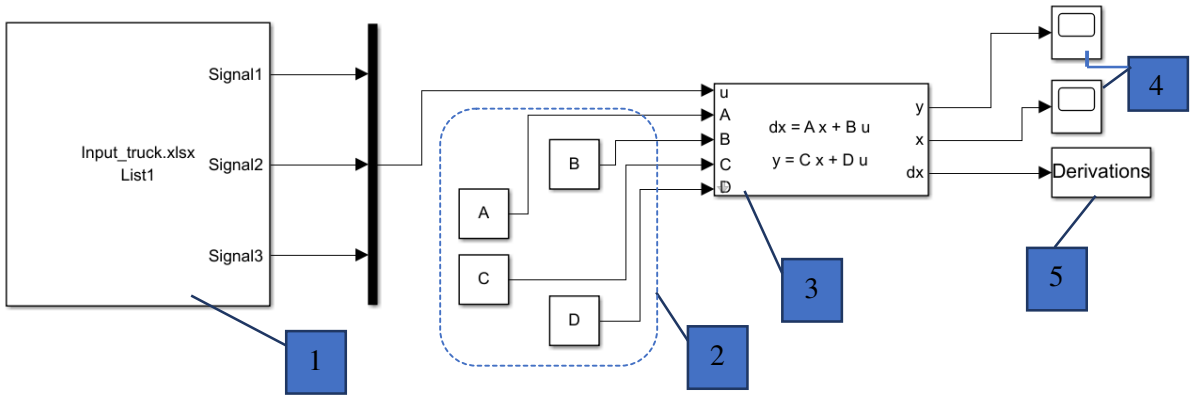

Fig. 4. **Simulink diagram of the state-space model with corresponding blocks:** 1 – data load from the spreadsheet, time is not considered as signal; 2 – constants loaded from the workspace, matrices of the state-space, 3 – varying state-space block that enables export of the second derivations, 4 – scopes utilized for the data display for the control purposes, 5 – block that enables data saving into the workspace for further export

9 DOF vehicle model

For the tandem rear axles, the top part of the vehicle remains unchanged, to the bottom part is added the massless beam, which is pivoted to the chassis of the vehicle. This beam has the pitch motion, therefore the model gains one additional DOF – equation (9). The governing equations (3-6) are the same as in the previous section,the restis a bit different (1c), (2c), (7c), (8c).Additional labels stand for: φ_{Ls} the pitch angle of the beam (rad), $\dot{\varphi}_C$ its velocity (rad·s^{-1}) and $\ddot{\varphi}_C$ its aceleration (rad·s^{-2}), $x_{LLs1,2}$ is the vertical displacement of the beam at the end, where it meets the suspension (m), its velocity x_{LLs2} respectively (m·s^{-1}) and I_{Ls} is the pitch axis moment of inertia of the beam (kg·m^2). The rest of the labels are the distances in (m). The equations were solved exactly like in the previous section – Fig. 4.

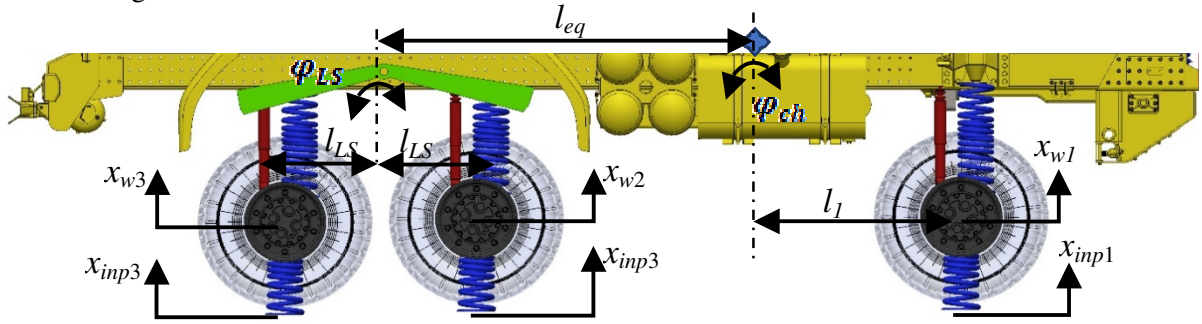

Fig. 5. **Half truck schematic system with the tandem rear suspension – bright green is the beam element**

$$m_{ch}\cdot\ddot{x}_{ch} = k_{S1}\cdot(x_{w1} - x_{ch1}) + c_{S1}\cdot(\dot{x}_{w1} - \dot{x}_{ch1}) + k_{C1}\cdot(x_{chC1} - x_{C1}) -$$
$$- c_{C1}\cdot(\dot{x}_{chC1} - \dot{x}_{C1}) - k_{C2}\cdot(x_{chC2} - x_{C2}) - c_{C2}\cdot(\dot{x}_{chC2} - \dot{x}_{C2}), \quad (1c)$$

$$I_{ch}\cdot\ddot{\varphi}_{ch} = l_1\cdot k_{S1}\cdot(x_{w1} - x_{ch1}) + l_1\cdot c_{S1}\cdot(\dot{x}_{w1} - \dot{x}_{ch1}) - l_4\cdot k_{C1}\cdot(x_{chC1} - x_{C1}) -$$
$$- l_4\cdot c_{C1}\cdot(\dot{x}_{chC1} - \dot{x}_{C1}) + l_5\cdot k_{C2}\cdot(x_{chC2} - x_{C2}) + l_5\cdot c_{C2}\cdot(\dot{x}_{chC2} - \dot{x}_{C2}), \quad (2c)$$

$$m_{w2}\cdot\ddot{x}_{w2} = k_{t2}\cdot(x_{inp2} - x_{w2}) - k_{Ls}\cdot(x_{w2} - x_{LLs1}) - c_{Ls}\cdot(\dot{x}_{w2} - \dot{x}_{LLs1}), \quad (7c)$$

$$m_{w3}\cdot\ddot{x}_{w3} = k_{t3}\cdot(x_{inp3} - x_{w3}) - k_{Ls}\cdot(x_{w3} - x_{LLs2}) - c_{Ls}\cdot(\dot{x}_{w3} - \dot{x}_{LLs2}), \quad (8c)$$

$$I_{Ls}\cdot\ddot{\varphi}_{Ls} = l_{Ls}\cdot k_{Ls}\cdot(x_{w2} - x_{LLs1}) + l_{Ls}\cdot c_{Ls}\cdot(\dot{x}_{w2} - \dot{x}_{LLs1}) - l_{Ls}\cdot k_{Ls}\cdot(x_{w3} - x_{LLs2}) -$$
$$- l_{Ls}\cdot c_{Ls}\cdot(\dot{x}_{w3} - \dot{x}_{LLs2}) \quad (9)$$

where $x_{LLs1} = l_{Ls}\cdot\varphi_{Ls}$, $x_{LLs2} = -l_{Ls}\cdot\varphi_{Ls}$.

Results and discussion

Presented in Fig. 6 are the results of the comparative analysis, it is obvious that as expected, this simple model is not able to represent the behaviour of equalizing beam suspension. As mentioned before, by decoupling the rear tandem from the rest of the vehicle, the vertical motion of the chassis, shades of blue colour, is for the solid line stable after the first excitation and a while. Second and third excitation have no effect. On the other hand, for the 8DOF model, dashed line, the effect of the second and third excitation is obvious. Analogically, the same rule is applied for the displacement of the cabin and seat. The coefficients and constants remained the same for 8 and 9 DOF models.

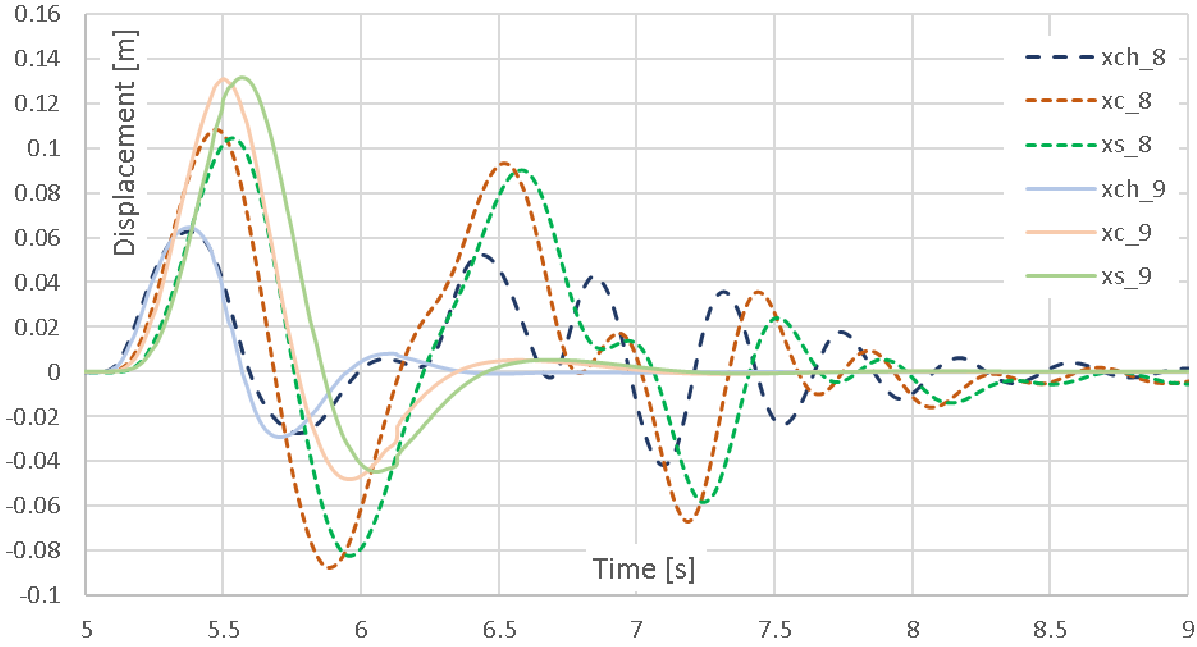

Fig. 6. **Graphical representation of vertical displacement changes of the chassis, seat, cabin for 8/9 DOF**

The duration of simulation was 25 seconds, by this time the second and third wheels were stable, however, it takes too long due to low linearized damping of the leaf spring and neglected friction in the pivot point. The independent suspension for 8DOF model behaved as expected.

Tandem suspension is too complex for the basic state-space simulation; satisfactory results can be obtained from the multi-body simulation [8]. Model with 10 DOF was conducted and simulated, but the results were even worse – the stiff spring was inserted between the beam and chassis, to secure the transfer of the forces between the tandem and chassis.

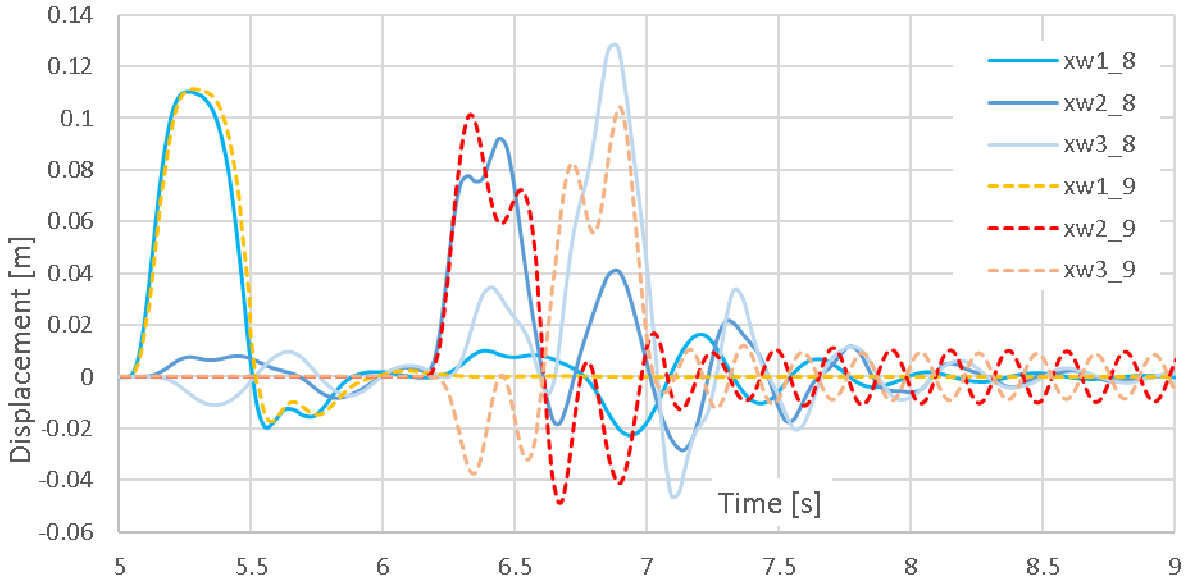

Fig. 7. **Graphical representation of vertical displacement of the unsprung masses for 8/9 DOF**

Conclusions

Two different approaches for the state-space models of the half truck were presented and evaluated. The biggest drawback of the state-space models is the extremely complex implementation of the nonlinear characteristics for the damper and spring elements. Therefore, they were linearized and afterwards used as the relevantcoefficient. In terms of off road manoeuvres, the overcoming of a relatively small bump was a simple task for the suspension, so the bump-stops could be neglected. For "worse" excitations they would have to be implemented due to their irreplaceable task within the suspension system.

For the future research, the beam in the tandem system should be replaced by something more complex and deformable, the amount of DOF should be sufficient, but the tandem system must beaccordingly coupled with the chassis, so the forces and displacements can be transferred between the two. The equalizing tandem suspension system should able to reduce the vertical motion of the chassis caused by the bump by half, unfortunately, the state-space systems with 8,9 and 10 DOF failed to do so.

Acknowledgements

The presented paper has been prepared with the support of the Ministry of Defence of the Czech Republic, Partial Project for Institutional Development, K-202, Department of Combat and Special Vehicles, University of Defence, Brno.

References

[1] Hegazy S., Sharaf A. M. Ride Comfort Analysis Using Quarter Car Model. International Conference on Aerospace Sciences and Aviation Technology 2013, [online] [30.03.2020]. Available at: http://asat.journals.ekb.eg/article_22238.html

[2] Sun, T., Zhang, Y., and Barak, P., "4-DOF Vehicle Ride Model," SAE Technical Paper 2002-01-1580, 2002, [online] [29.03.2020]. Available at: https://www.sae.org/publications/technical-papers/content/2002-01-1580/

[3] Mohmammadi Y.,Ganjefar S. Quarter car active suspension system: Minimum time controller design using singular perturbation method. International Journal of Control, Automation and Systems [online]. 2017, 15(6), pp. 2538-2550 [online] [26.3.2020]. Available at: http://link.springer.com/ 10.1007/s12555-016-0608-3

[4] Liu H., Gao H., Li P. Handbook of vehicle suspension control systems. London: The Institution of Engineering and Technology, 2013. ISBN 978-1-84919-633-8.

[5] Maloch M., Cornak S.Multileaf Spring Model and Its Behaviour in a Tandem Bogie Layout.International Conference on Civil, Structural and Transportation Engineering 2019, [online] [27.03.2020]. Available at: http://avestia.com/ICCSTE2019_Proceedings/files/paper/ICCSTE_191.pdf
[6] Jayakumar P., Alanoly J., Johnson R."Three-Link Leaf-Spring Model for Road Loads" SAE Technical Paper 2005-04-11, [online]. [29.03.2020]. Available at: https://www.sae.org/content/2005-01-0625/
[7] SS: State-space model, Https://www.mathworks.com/ [online] [30.03.2020]. Available at: https://www.mathworks.com/help/control/ref/ss.html
[8] Yang Y., Ren W., Chen L., Jiang M.etc. Study on ride comfort of tractor with tandem suspension based on multi-body system dynamics. Applied Mathematical Modelling [online]. 2009, 33(1), 11-33 [30.03.2020]. Available at: https://linkinghub.elsevier.com/retrieve/pii/S0307904X0700265X